Eur. Phys. J. E **33**, 41–49 (2010)
DOI 10.1140/epje/i2010-10657-4

THE EUROPEAN PHYSICAL JOURNAL E

Regular Article

Thin film polymer photonics: Spin cast distributed Bragg reflectors and chirped polymer structures

J. Bailey and J.S. Sharp[a]

School of Physics and Astronomy and Nottingham Nanotechnology and Nanoscience Centre, University of Nottingham, Nottingham, NG7 2RD, UK

Received 16 July 2010
Published online: 25 September 2010 –

Abstract. Polymer based photonic structures were produced by spin coating up to 50 alternating layers of polystyrene (PS) and poly(vinylpyrrolidone) (PVP) from mutually exclusive (orthogonal) solvents. The resulting thin film multi-layer structures were studied using a simple optical reflectivity apparatus and were shown to have narrow (10–20 nm wide) reflectance bands in the visible region. The position of the reflectance bands was controlled by varying the spin speed used during production of the multi-layers and peak reflectance values of 55% were obtained for samples containing 50 layers. The results were shown to be in agreement with modified optical transfer matrix method calculations which include the effects of diffuse polymer interfaces. This modelling approach revealed that the width of the polymer/polymer interfaces formed by spin coating was in the range 15–20 nm. Data and calculations were also obtained for chirped polymer photonic structures. These results were also shown to be in good agreement. These experiments demonstrate that simple processing methods such as spin coating can be used to produce organic photonic structures with tailored optical properties.

1 Introduction

Photonic crystals are composite materials that contain spatial modulations in their refractive index. When the period associated with these spatial modulations is comparable to the wavelength of light, interference effects cause specific wavelengths to be preferentially reflected and give rise to some interesting optical effects [1]. The periodicity in refractive index causes a photonic band gap to appear in the measured optical response of the structures [1] and the optical properties of a photonic crystal can be controlled by simply changing the periodicity of the structure and/or the magnitude of the refractive index variations within the structure. The relative simplicity associated with the production of photonic crystals has resulted in their finding applications in the manufacture of optical filters [2], resonant cavity LEDs [3], solar cells [4] and lasers [5–9]. These structures also have potential applications in acousto-optical devices [10].

Photonic crystals are also ubiquitous in natural systems. For example, topographical surface structures with periodic variations in refractive index can be found on the wings of Morpho butterflies [1]. The shells of molluscs and the scales of fish have also been shown to contain periodic layered structures that preferentially reflect light over a desirable range of wavelengths [1,11]. In the case of many animals, birds and insects the photonic structures that are formed have numerous applications and have been selected to create a wide range of structural colours and reflection phenomena. These modifications have been adapted and used by biological organisms to either attract a mate, to lure prey or to confuse and avoid predators. Some plants have also been shown to use simple photonic structures in their leaves which act as micro-lenses. These structures act to focus incoming light on to chloroplasts and hence improve the efficiency of photosynthesis [9].

Numerous attempts have been made to manufacture artificial photonic crystals and to mimic some of the properties of natural systems [1]. The techniques that have been employed include the use of self-assembling colloidal particles [12], layer-by-layer deposition and growth of materials [5–9] and top-down lithographic techniques [13]. However, the simplest form of photonic crystal can be made by simply depositing alternating layers of two or more dielectric materials that have different refractive indices to produce a thin film multi-layer structure. These samples are often referred to as dielectric mirrors.

When light is incident upon an interface between two dielectric materials (such as a glass/air or a polymer polymer interface) a certain amount will be reflected and the rest will be transmitted. If many of these dielectric interfaces are stacked parallel to one another, then incident light will undergo many reflections and the layered structure will reflect much more light than a single interface.

[a] e-mail: james.sharp@nottingham.ac.uk

Moreover, if the thickness of the layers in the stack is held constant so that the interfaces are separated by a distance that is comparable to the wavelength of light, constructive interference effects within the layered structure will result in certain wavelengths being preferentially reflected. This type of stratified multi-layer structure is often referred to as a distributed Bragg reflector (DBR) [2,8] and the optical response of these simple photonic crystals can be controlled by simply varying the individual layer thicknesses. These simple layered structures are used widely in the manufacture of commercial optoelectronic devices such as the lasers that are found in CD and DVD players.

There are two main strategies that can be adopted in the manufacture of simple DBR structures. The first of these is to use relatively few layers where the optical contrast (difference in refractive index) between layers is relatively high. The second is to use many layers with small amounts of optical contrast between them. Each method has its own advantages and disadvantages. Many researchers have opted to use the first approach as this requires the deposition of fewer layers, resulting in a lower number of potential defects within the final structure [1,7]. This approach necessitates the use of inorganic materials [14] or inorganic/organic hybrid structures [7] and results in structures that have wide photonic band gaps. The main disadvantage of this approach is that it often requires the use of costly manufacturing methods such as vacuum deposition techniques or liquid phase epitaxy based methods and the raw materials that are used to produce the structures can be highly toxic.

Organic materials such as polymers present a number of attractive routes for the manufacture of photonic structures. However, the small contrast differences that occur at polymer/polymer and polymer/air interfaces lead to lower reflectance values than those obtained from inorganic materials. As a result of this, many more repeat units must be introduced into the photonic structure to obtain the desired peak reflectance values and this can be seen as a disadvantage. This potential problem can be offset by the fact that polymers can be quickly and easily processed using melt casting [8] or solvent based techniques such as spin coating [9,15]. These solvent and melt casting based approaches can also be more attractive than methods that use the self-assembly of block copolymers [6] as there is no need to introduce a specialized synthesis step to obtain the desired layer thickness values in the multi-layer structures that are formed. The layer thickness values can simply be controlled by changing simple processing parameters.

Another feature of polymer based photonic structures is that they have significantly narrower reflection bands than those observed in inorganic and inorganic/organic hybrid structures [2,16]. This occurs because of the small amounts of optical contrast that exist between transparent organic materials. For example, typical values of the refractive indices of polymers fall in the range 1.4–1.6 [17]. These low levels of contrast are a disadvantage if the desired effect is to create a broad band reflector but they represent a significant advantage in the manufacture of optical components such as notch filters and dichroic mirrors where narrow reflection bands are required. Narrow reflection bands are also advantageous in acousto-optic modulators where small applied mechanical strains can be used to change the size of the domains/layers in the photonic structure. This causes small changes in the periodicity of the structure and a shift in the main reflectance peaks. These changes in periodicity give rise to large changes in reflected intensity in the spectral region occupied by the main reflectance bands.

A key requirement in the production of any multi-layer DBR structures is that the deposition of new layers does not interfere with previous layers in the structure. Although this is not usually a problem during the deposition of inorganic materials, this can be a concern when using polymers. This is because the materials are often similar in their chemical composition, *i.e.* a chain with a carbon backbone that is decorated with different functional groups. A result of this similarity in structure is that these materials will often form broad interfaces with other polymers. More importantly, the solvent for one polymer can often dissolve or swell other polymers. When solvent casting multi-layer structures swelling effects can result in the dissolution, or disruption of previous layers in the structure when a new layer is deposited. However, these effects can be circumvented if great care is taken to choose immiscible polymers and appropriate mutually exclusive (or orthogonal) solvents when building the structures [2,16].

In this paper, we describe an experimental study of the angular dependent optical properties of thin film polymer multi-layer (DBR) structures that were spin coated from solutions of polystyrene (PS) and poly(vinylpyrrolidone) (PVP) in toluene and ethanol/acetonitrile blends, respectively. We show that the resulting structures have narrow reflectance bands in the visible region and that the reflectance properties of these samples can be accurately modelled using a simple optical transfer matrix method which incorporates the effects of diffuse polymer/polymer interfaces. Data and calculations are also presented for chirped polymer photonic structures that are prepared using a computer controlled spin coater. To the best of our knowledge these combined experiments and diffuse interface calculations are the first of their kind. This combined approach allowed us to extract information about the interfacial widths of polymer/polymer interfaces that are formed by spin coating. Moreover this was done using a simple optical technique. This information is usually obtained using more expensive techniques such as neutron (or X-ray) reflectivity studies or ion beam methods [18]. We therefore anticipate that this work will be of interest to physicists, physical chemists and materials scientists that study thin films and interfaces in soft condensed matter systems. This study also represents the first report of spin cast chirped thin film polymer multi-layer structures. Automation of the spin coating process allowed us to vary the thickness values of the layers in the photonic structure in a controlled way. This has enabled us to produce low-cost organic photonic materials with tailored optical properties.

2 Experimental

Alternating layers of PVP (average M_w = 1300 kDa, BASF, Germany) and PS (Average M_w = 192 kDa, Sigma, UK) were spin coated on to clean glass microscope slides (75 mm × 25 mm) from 4 wt% solutions in ethanol/acetonitrile (50/50 weight ratio) and toluene, respectively. In each case, PVP films were deposited first and samples with 10, 20, 30, 40 and 50 alternating layers of PVP and PS were deposited on to different glass substrates. Following the deposition of each PVP layer, the samples were exposed to concentrated hydrochloric acid (HCl) vapour. This treatment swells the PVP layers, preventing organic solvents from passing through them and disrupting the underlying multi-layer structure when new layers are deposited.

The thickness values of the individual layers in the DBR multi-layer structures were controlled by varying the spin speed between 1100 and 2500 rpm during deposition of the films. All samples were prepared using a purpose-built computer controlled spin coater. Chirped photonic samples were also prepared using the same spin coater. Each of these chirped samples contained a total of 50 layers. The thickness of the first PS and PVP layers was set at the desired value and the thickness of the PS and PVP layers was incremented in steps of a few nanometres in subsequent periods of the chirped multi-layer structures.

All the multi-layer samples were annealed under vacuum (∼ 1 mtorr) for 5 hours at 110 °C to remove residual solvent and stresses that may have been introduced into the multi-layers during the spin coating procedure. The glass transition temperatures of PS and PVP are 97 °C and 170 °C, respectively [17]. Annealing the samples above the glass transition temperature of PVP was not possible as the samples were found to degrade at temperatures above 150 °C. Following annealing, the samples were allowed to cool to room temperature before the optical transmission/reflection properties of the samples were measured as a function of the angle of incidence, θ, for values of $0° < \theta < 45°$. These measurements were performed using a home-built optical apparatus comprising a tungsten halogen lamp, a sample holder mounted on a rotation stage and a RedTide USB650 fibre optic spectrometer (Ocean Optics, see inset fig. 1). The spot size used to probe the optical properties of the samples had a diameter of 6 mm. However, the optical response was found to be uniform over large areas of the sample (25 mm × 25 mm). The samples were also inspected using an Olympus BX51 optical microscope. Inspection revealed that the multi-layer samples were uniform in colour over large areas and contained very few defects (see inset fig. 2). These observations are consistent with those made on single films of PS and PVP that were spin coated on to similar glass substrates and they are also consistent with the uniform optical response of the samples.

Despite the fact that both PS and PVP are transparent materials, the periodic changes of the refractive index in the multi-layer samples caused them to preferentially reflect certain wavelengths of light in the UV/visible region. All optical measurements were performed in a transmission geometry and the transmittance, T (%), was obtained by taking a ratio of the transmitted and incident intensities of light at each wavelength and multiplying by 100. The reflectance, R (%), was then calculated using the relationship $R = 100 - T$. This assumes that there is no absorption of light in the materials used over the wavelength range being studied. Optical measurements of glass, PVP and PS layers of different thickness values confirmed that no absorption occurred in these material over the 400–1000 nm wavelength range.

Measurements of the wavelength dependence of the refractive index of the glass substrates and the PS and PVP layers were performed using a Woollam M2000V spectroscopic ellipsometer (see inset fig. 1). The refractive indices for these materials were found to be consistent with

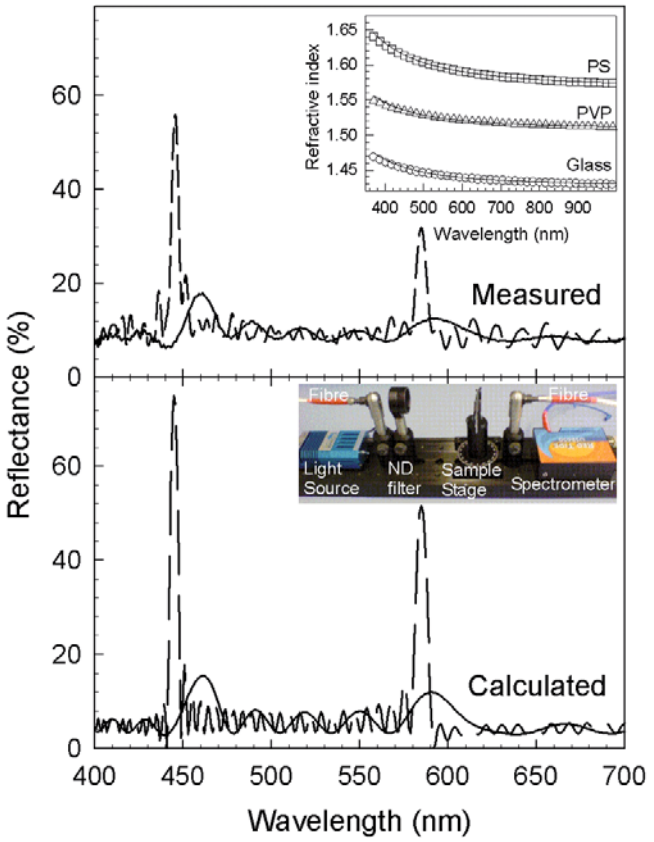

Fig. 1. Wavelength dependence of the reflectance of PS/PVP multi-layers measured at normal incidence. The top panel shows measured data collected from blue/violet reflecting DBR samples. The bottom panel shows the results of transfer matrix calculations that were performed by assuming perfectly sharp interfaces between successive PS and PVP layers. Each panel shows data/calculations for samples with 10 (solid line) and 50 (dashed line) layers. The inset in the top panel shows data for the wavelength dependence of the refractive index of PS, PVP and glass. The solid lines in this plot represent the fits to eq. (1) that were used to parameterise the refractive index in the transfer matrix calculations. The thickness values that were used in the calculations are summarised in table 2. The inset in the bottom panel shows a photograph of the apparatus used to measure the optical properties of the samples.

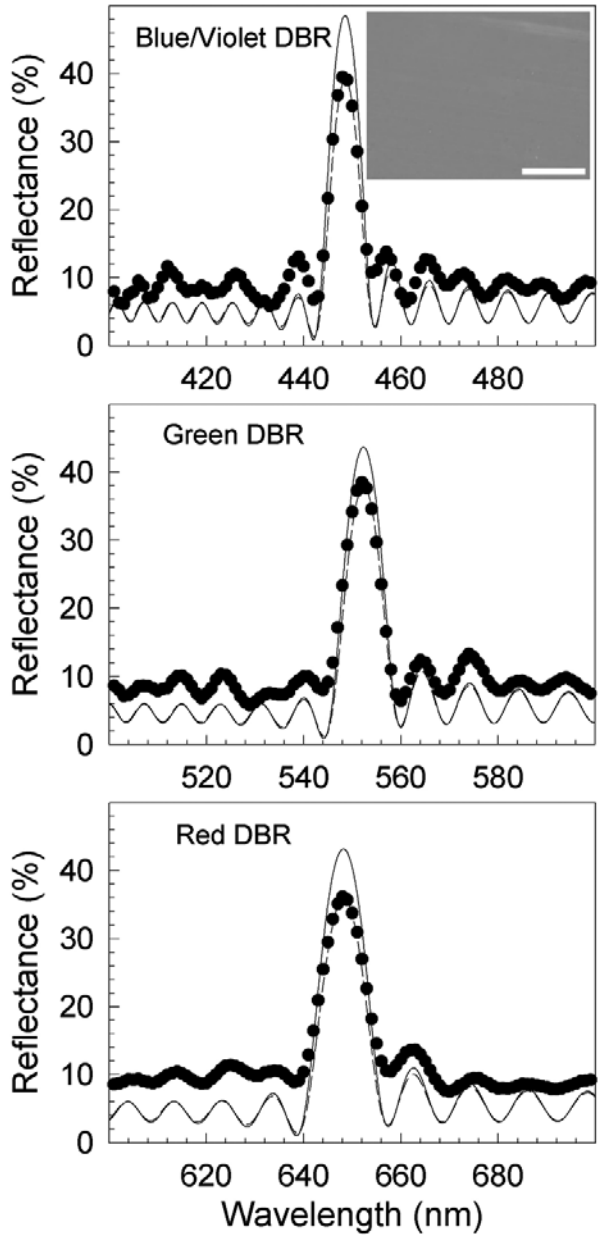

Fig. 2. Wavelength dependence of the reflectance of different coloured PS/PVP multi-layers. Data are shown for a blue/violet (top panel), green (middle panel) and red (bottom panel) reflecting DBRs with 30 layers at normal incidence. In each panel, the circles represent measured data and the solid lines show the results of transfer matrix calculations that assume sharp interfaces between the PS and PVP layers. The dashed lines show the results of similar calculations that include the effects of diffuse polymer/polymer interfaces. The values that were used for the individual layer thickness values and the widths of the interfaces in these calculations are given in table 2. The inset in the top panel shows an optical micrograph of blue/violet DBR surface (scale bar: 1 mm).

literature values [17]. The thickness of the polymer layers was determined by spin coating solutions of the same polymers on to single crystal silicon wafers using identical deposition parameters to those used during the manufacture of the multi-layers. These samples were then annealed and their thickness was determined using a home-built self-nulling ellipsometer (wavelength $\lambda = 633\,\text{nm}$). Thickness values were found to lie in the ranges 328–486 nm for PVP and 212–310 nm for PS.

The root mean square (r.m.s.) roughness of the multi-layer samples was also measured using an Asylum Research MFP-3D scanning force microscope (SFM) operating in intermittent contact mode. SFM scans were collected at several positions on the surface of each of the multi-layer samples using scan sizes of $40\,\mu\text{m} \times 40\,\mu\text{m}$. The SFM measurements showed no evidence of defects or large scale in-plane structure on the samples other than that caused by the natural r.m.s. roughness associated with spin coating. Measurements of the r.m.s. surface roughness, σ_{surf}, for the samples were determined to lie in the range $1.2 \pm 0.4\,\text{nm}$ to $4.1 \pm 0.3\,\text{nm}$. The increases in roughness observed from sample to sample was consistent with an increase in individual layer thickness within the samples and is similar to that obtained from single spin cast polymer films. The low measured roughness values demonstrate that the surfaces of the samples are flat on optical length scales. This observation is consistent with the presence of the uniform colours that were observed on these samples.

A transfer matrix model [19] was then used to model the wavelength dependence of the reflectance (R) of the polymer multi-layer samples at different angles of incidence (θ). These calculations included a model which assumed perfectly sharp interfaces between the layers and a model which includes the effects of diffuse polymer/polymer interfaces. In the case of the sharp interface model, only the layer thickness values and the wavelength dependence of the refractive indices of PVP, PS and glass (obtained from ellipsometry measurements) were used to generate the wavelength dependence of the optical reflectance. The interfacial width of the polymer/polymer interfaces (σ) was introduced as an adjustable parameter in the diffuse interface model.

3 Results and discussion

Figures 1 and 2 show the wavelength dependent reflectance of three different PS/PVP polymer multi-layer DBR structures measured at normal incidence. These three samples had reflectance bands (photonic bandgaps) in the blue/violet (440–460 nm, fig. 1 and fig. 2 (top panel)), green (540–560 nm, fig. 2, middle panel) and red (640–660 nm, fig. 2, bottom panel) regions of the visible spectrum. The top panel of fig. 1 shows reflectance data obtained from samples with 10 and 50 layers and the bottom panels show the results of calculations for the same numbers of layers that were performed using a simple transfer matrix method [19,20]. In this simple matrix method, each interface is assumed to be perfectly sharp and is represented by a single 2×2 reflection matrix whose elements are comprised of the relevant combinations of the Fresnel reflection and transmission coefficients

Table 1. Cauchy fit parameters used to model the wavelength dependence of the refractive indices of PVP, PS and glass (see eq. (1) and fig. 1).

Parameter	PVP	PS	Glass
a	1.5085 ± 0.0005	1.5665 ± 0.0005	1.4275 ± 0.0005
b (nm^2)	2947 ± 177	7200 ± 115	2864 ± 122
c (nm^4)	5.000 ± 0.241	5.000 ± 0.156	5.000 ± 0.167

(r and t, respectively) for that interface [19,20]. Transmission through each layer introduces a small phase change to the incident light which is represented by a 2×2 transmission matrix. The 2×2 reflection matrix for the entire DBR is then calculated by simply multiplying the reflection and transmission matrices for all the layers together. The reflectance of the structure is then calculated using the relevant elements in the final 2×2 matrix. In all the calculations that are described below the wavelength dependence of the refractive indices of the PS, PVP and the glass substrates used to make the polymer DBR structures were incorporated into the model by fitting the refractive index values obtained from ellipsometry (see inset in the top panel of fig. 1) to the Cauchy formula

$$n = a + \frac{b}{\lambda^2} + \frac{c}{\lambda^4}\,, \tag{1}$$

where a, b and c are fit coefficients and λ is the wavelength of light (in nm, see table 1). The values of a, b and c obtained from fits to eq. (1) were used to parameterise the wavelength dependent refractive index of each of the layer materials when calculating the Fresnel reflection and transmission coefficients of each of the interfaces in the multi-layer samples.

The values of the PVP and PS layer thickness that were used in the calculations of the reflectance spectra shown in figs. 1 and 2 are given in table 2. As this table shows, the thickness values that were used to obtain agreement between the positions of the measured and calculated reflectance peaks are up to 30 nm higher than the measured values that were obtained from equivalent individual spin cast layers deposited on Si wafers. The discrepancy between the measured and calculated PVP and PS layer thickness values is attributed to the fact that the layers in the DBRs are spin coated onto underlying polymer layers and not Si wafers. We anticipate that the thickness values that are obtained for a given set of deposition parameters will be slightly different on polymer surfaces due to differences in the wetting properties of Si wafers, PS and PVP surfaces for the solutions being used to deposit the layers. Accurate determination of the thickness of a polymer layer that is spin cast on top of another polymer is also extremely difficult due to the diffuse nature of the polymer/polymer interfaces that are formed during spin coating (as discussed below). The differences between the measured thickness and the thickness values used in the calculations are therefore not a cause for concern. The measured PS and PVP film thickness that are given in table 2 should be used only as a guide to the true layer thickness values in the multi-layer structures. However, the level of agreement between the shapes of the measured and calculated reflectance spectra shown in figs. 1 and 2 is extremely encouraging and gives us confidence that the measured thickness values are close to the layer thickness values used in the calculations.

The measured and calculated values of the peak reflectance shown in figs. 1 and 2 are clearly different. Values of the peak reflectance for samples with different numbers of layers are summarised in fig. 3, where measured (solid symbols) and calculated (lines) values of the peak reflectance, $R(n)$, are plotted as a function of the number of layers (n) for the three polymer DBR multi-layer structures. In each case, the measured value of $R(n)$ is lower than that predicted by the calculations, but the functional form associated with the calculated and measured $R(n)$ curves appears to be similar. It is noteworthy that the measured reflectance values in fig. 3 do not appear to have reached their maximum value even after 50 layers and the value of $R(n)$ is still increasing. This indicates that samples with higher peak reflectance values could be obtained by increasing the number of layers in the multi-layer DBR stacks.

The simple transfer matrix model that was used to calculate the reflectance values shown in figs. 1 to 3 assumes that the interfaces between neighbouring layers are perfectly sharp and hence that there is abrupt change in the refractive index profile from that of PVP to PS (or vice versa) at each interface. This is unlikely to be the case for the samples studied here and would explain why the measured peak reflectance values are lower than the calculated values. The reason for this is that polymer/polymer interfaces that are formed during spin coating are expected to have interfacial widths as large as 10 nm [21], caused by the mixing of the polymers at the interface. This will have the effect of broadening the interface and producing a continuously varying refractive index profile in the interfacial regions. A result of this interfacial broadening is that the amount of light which is reflected at a given interface will be reduced. In fact, any roughness, diffuseness or in-plane structure associated with the interfaces will also cause an effective smearing out of the interfacial region and will result in deviation from the ideal step-like change in refractive index assumed in the simple transfer matrix model and giving rise to a reduction in reflectance.

Decoupling the effects that roughness and diffuse interfaces have upon the measured reflectance properties of the multi-layers can be difficult. However we note that SFM measurements of the multi-layer sample surfaces gave r.m.s. roughness values of a few nanometres. Calculations show that roughness on the nanometre length scale does not significantly influence the optical reflection properties of a polymer/polymer interface but that diffuseness on the lengthscale of tens of nanometres does affect the reflectance spectra. When incorporating these effects, both roughness and diffuseness are often treated in exactly the same way. This is done by introducing Gaussian smooth-

Table 2. Parameters used in the transfer matrix calculations.

DBR	Measured PVP thickness on Si (nm)	PVP thickness used in calculations (nm)	Measured PS thickness on Si (nm)	PS thickness used in calculations (nm)	σ (nm) Diffuse interface calculations
Blue/Violet (440–460 nm)	328 ± 1	336 ± 8	212 ± 1	223 ± 11	15 ± 1
Green (540–560 nm)	396 ± 1	411 ± 15	256 ± 1	271 ± 15	15 ± 1
Red (640–660 nm)	486 ± 1	496 ± 10	310 ± 1	320 ± 10	20 ± 1

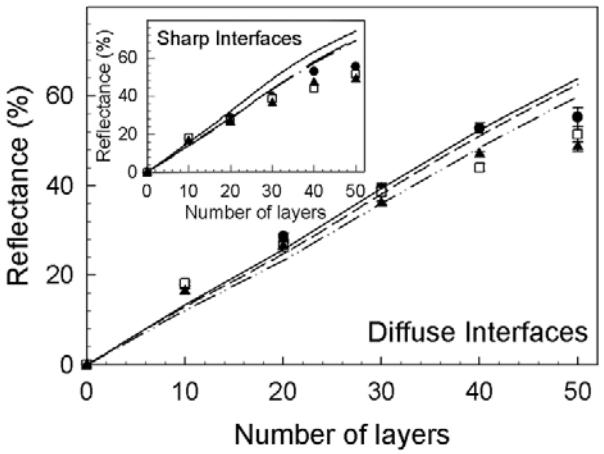

Fig. 3. Variation in the peak reflectance with the number of layers. Data are shown for maximum reflectance of the dominant peak in the spectra for blue/violet (circles), green (squares) and red (triangles) DBR multi-layers, respectively. The main panel shows the results of transfer matrix calculations that include the effects of diffuse polymer/polymer interfaces. The inset shows a comparison between data and the results of similar calculations that were performed using sharp interfaces. The thickness and interfacial width values that were used in these calculations are summarised in table 2.

ing parameters that modify the Fresnel reflection coefficients for abrupt interfaces (r). The modified reflection coefficients, r_{rough}, typically take the form [18,20,22]

$$r_{\text{rough}} = r \exp\left(-\frac{8\pi^2 n_{\text{inc}}^2 \sigma^2}{\lambda^2}\right), \qquad (2)$$

where λ is the wavelength of the incident light, σ is the interfacial width and n_{inc} is the refractive index of the incident layer. The corresponding transmission coefficients at each interface are then modified by ensuring that energy is conserved, *i.e.* that any incident light that is not reflected at the interface is transmitted.

Optical transfer matrix calculations were also performed on multi-layers with rough interfaces using the modified Fresnel coefficients given in eq. (2). The value of σ that was used in the calculations was varied to obtain the best fit to the $R(n)$ curves shown in fig. 3 for each colour of DBR studied. Figures 2 and 3 show the results of the diffuse interface calculations and the values of σ that were used in the calculations are given in table 2. The values obtained for σ fall in the 15–20 nm range. These are comparable to (but slightly larger than) values that have been reported for the measured interfacial widths of spin cast polymer/polymer interfaces [21]. Moreover, the results of the calculations suggest that the width of the interface may increase slightly with increasing PS and PVP thickness values. Although not entirely conclusive, such an observation is consistent with neutron reflectivity measurements of the equilibrium interfacial width in bi-layers of other polymers [18]. However, while the level of agreement between the data and these new calculations are encouraging, we must take care not to over interpret the diffuse interface calculations. The width of the interface between PS and PVP is likely to depend upon the order in which the two repeating layers within the structure are deposited. The details of the interfacial structure are likely to be different for a PS/PVP interface than a PVP/PS interface because the uppermost layer is deposited from a different solvent in each case. The reason for this is that the solvents used here are unlikely to be a perfect mutually exclusive (orthogonal) system and are likely to generate different amounts of swelling in the layers for which they are supposed to be non-solvents. Although the extent of swelling of underlying layers is small enough to prevent disruption of the DBR structure, it may be sufficient to change the details of the interfacial structure and give rise to two types of interface, each having a different width value. At this point, we also recall that the samples were annealed at 110 °C to remove solvent and relax stress in the multi-layers while at the same time preventing degradation of the samples (which can occur at higher temperatures). This annealing temperature is below the glass transition temperature of PVP and hence the PVP polymer chains are unlikely to have relaxed sufficiently on the time scales associated with annealing (~ 5 hours). The samples are therefore unlikely to have been annealed long enough to form equilibrium PS/PVP interfaces with a single, well-defined width value. Based upon these arguments, the use of a single interfacial width in the transfer matrix calculations is too simplistic and the approach described above represents an approximation to the true interfacial structure in the DBR multi-layer samples that are studied here. The use of two different values would therefore seem more appropriate. However, in the absence of detailed measurements (such as neutron reflectivity data) of the interfacial width of the PS/PVP interfaces formed here, the exact nature of the contribution of broad interfaces to the wavelength dependent reflectivity of the

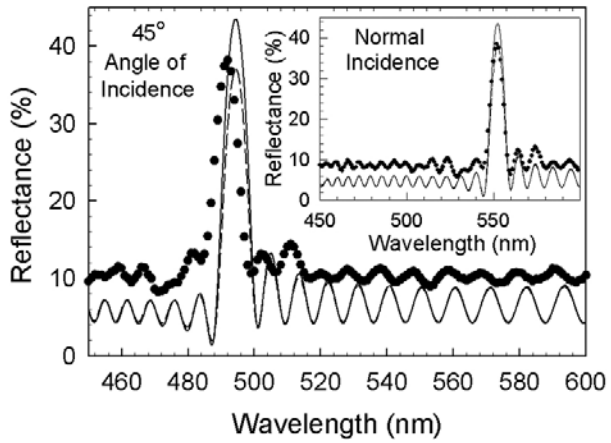

Fig. 4. Angular dependence of reflectance spectra. The main panel shows data for a 30 layer green (DBR) that was measured at a 45° angle of incidence. The inset shows data that was reproduced from fig. 2 for the same sample measured at normal incidence. Each plot contains measured data (circles) and the results of transfer matrix calculations that were obtained by assuming sharp (solid lines) and diffuse (dashed lines) polymer/polymer interfaces.

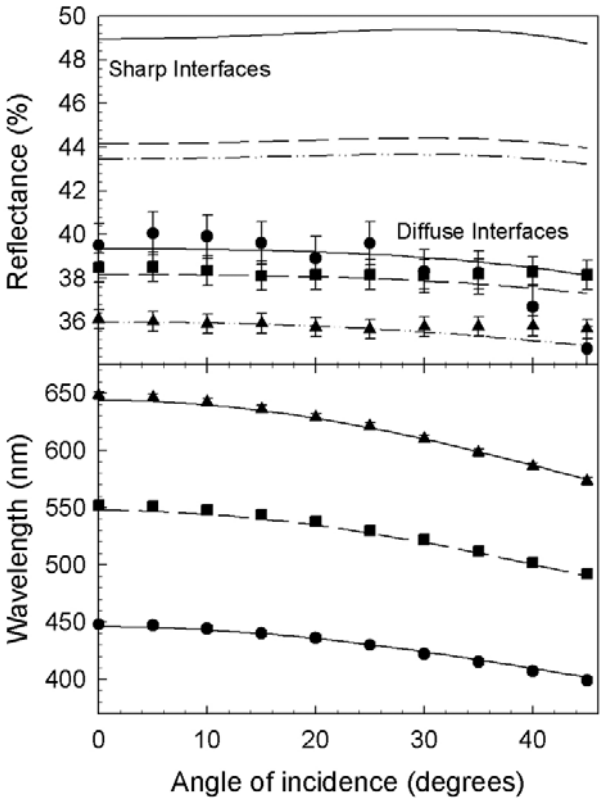

Fig. 5. Angular dependence of the reflectance and position of the dominant reflectance peak. Data and calculations are shown for blue/violet (circles), green (squares) and red (triangles) DBR multi-layer samples with 30 layers. The top and bottom panels show the variation of the reflectance and position of the dominant reflection peak, respectively. The lines show the results of transfer matrix calculations that were obtained for the blue/violet (solid), green (dashed) and red (dash-dot) multi-layers. In the top panel, the upper set of lines represent the results of calculations obtained for sharp interfaces and the lower set of lines are the result of diffuse interface calculations. In the bottom panel both sets of calculations produce identical results for the position of the dominant reflectance peak.

samples is difficult to quantify. This will be the focus of future studies.

The differences in the position of the baseline that are observed in figs. 1 and 2 are attributed to small differences between the measurement geometry and that used in calculations. A semi-infinite glass substrate was assumed in the calculations. This means that the effects of the back interface of the glass substrate are not included. Calculations of the reflectance of a single glass/air interface give values of 3–4% over the wavelength range studied and would account for the differences observed in the position of the baseline. The inclusion of this additional interface in the calculations would increase the value of the interfacial width parameter, σ, that is required to fit the data. While in principle these effects could have been included, such a step would add additional layers of complexity to the models used and would give rise to relatively small changes in the values of σ that are obtained from the fits. We believe that the simple approach used in the calculations captures the essential physics and also enables comparison between the shapes of the measured and calculated reflectance spectra.

Figure 4 shows reflectance spectra that were collected from a 30 layer green DBR at normal incidence (inset) and at an angle of incidence of 45°. This figure also shows the results of transfer matrix calculations with sharp and diffuse polymer/polymer interfaces. As this figure shows, an increase in the angle of incidence results in the main reflectance feature being blue-shifted and is accompanied by a small change in the peak reflectance value. These effects are summarised for the three different colour DBRs studied in fig. 5. The bottom panel in fig. 5 shows the variation in the position of the dominant peak with increasing angle of incidence for DBR samples with 30 layers. This figure clearly shows that the position of the peaks obtained from experiments is in very good agreement with the results of transfer matrix calculations. The calculated curves in the bottom panel of fig. 5 are the same for diffuse and sharp interfaces. This is because the position of the dominant reflectance peak is determined by the average layer thickness values and the refractive indices of PS and PVP and is insensitive to the diffuseness of interfaces on the length scales discussed above. However, as discussed above, the reflection and transmission coefficients at an interface are influenced by its width. This is clearly demonstrated again in the top panel of fig. 5. The lines at the top of this panel show the results of calculations that were obtained using abrupt/sharp interfaces and the lines in the bottom half of the panel represent the results obtained from transfer matrix calculations which include diffuse interfaces with values of σ that are given in table 2. This panel shows that for angles of incidence less than 30° the measured reflectance of the DBRs does not

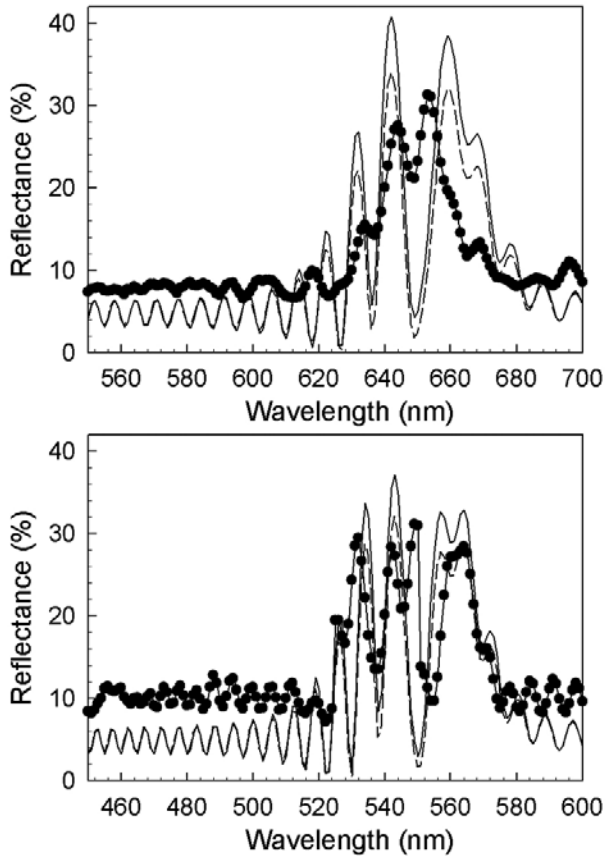

Fig. 6. Normal incidence reflectance spectra for chirped polymer samples. The top panel shows data collected from a 50 layer sample where the first two PVP and PS layers were fixed at a thickness of 300 nm and subsequent PS and PVP layers had their thickness values incremented by 1 nm. The bottom panel shows a similar plot for a 50 layer sample where the first two layers had thickness values of 250 nm and the thickness increment was 1 nm for successive periods within the structure. The solid lines show the result of transfer matrix calculations that assume sharp interfaces. The dashed lines are the results of diffuse interface calculations. The values of σ used in the diffuse interface calculations were 20 nm and 15 nm for the top and bottom panels, respectively.

change significantly. It also shows that the diffuse interface calculations are in good agreement with the measured reflectance values, but that there is some deviation of the data from the calculated curves above 30°. The reasons for this are not clear. However, given the relative simplicity of the modelling approach discussed above, the level of agreement between data and calculations is encouraging and provides additional evidence that the estimates obtained for the interfacial width and thickness values used are correct. These combined experiments and calculations also demonstrate that simple optical reflection techniques can provide information about the structure of interfaces on the tens of nanometres lengthscale.

The final set of experiments that were performed in this study involved the manufacture of chirped photonic DBR structures. In these samples the thickness of the first two PS and PVP layers was fixed at a known value and a computer controlled spin coater was used to increment the thickness of subsequent periods by a few nanometres. Calibration curves for the thickness *vs.* spin speed were obtained from measurements of single PS and PVP films on Si substrates. The calibration curves for both PVP and PS were then fitted to negative exponential functions and this information was used by the computer controlled spin coater to control the thickness of consecutive layers. Chirping the samples in this way effectively smears out the reflectance bands, giving rise to much broader peaks with lower reflectance values than those obtained for samples where the layer thickness values remain constant. These samples were also modelled using the transfer matrix calculations described above. Figure 6 shows examples of data that were collected from chirped polymer multi-layer samples. The top panel shows data and calculations for a sample where the thickness of the first two PS and PVP layers was set at 300 nm and the thickness of layers in subsequent repeat periods was incremented by 1 nm (top panel, sample A). This figure also shows data and calculations for a second sample (sample B, bottom panel) where the initial PS and PVP thickness was set at 250 nm and the thickness increment was 1 nm. The data clearly reproduces many of the features that are shown in the calculations (for sharp and diffuse interfaces) and chirping the multi-layer structures in this way clearly gives rise to broader reflectance features. The most likely reason for the small differences in the shape of the reflectance bands shown in fig. 6 is related to the precision with which the thickness of the individual layers in the structure can actually be controlled. The uncertainty associated with the film thickness of spin cast polymer films is typically greater than or equal to ± 1 nm. This means that we are unlikely to be able to control the thickness of each layer to within the 1 nm precision required for the chirped samples discussed here. However, despite this experimental limitation, the agreement between experiment and calculations is extremely good.

In summary, we have described a combined experimental and calculation based approach which enables the manufacture of polymer based photonic structures with tailored optical properties. This approach can also be used to obtain information about the structure of polymer/polymer interfaces in spin cast multi-layer samples. The multi-layer structures have potential applications in the manufacture of all polymer resonant cavity LEDs [3, 16] and we have also recently demonstrated their application as hypersonic crystals and acousto-optic modulators [10]. If the peak reflectance values of the multi-layers can be increased further —either by the inclusion of more layers or by the use of polymers with larger refractive index contrast— these structures would have potential applications for use as the mirrors in all-polymer lasers [6]. Clearly, the techniques described here result in the production of photonic structures with relatively small sample areas (25 mm $\times$ 25 mm) and while there is some possibility of scaling up the automated spin coating process, more attractive methods for the production of these multi-layer structures may lie in the use of so called roll-to-roll manufacturing processes or extrusion based techniques [8].

4 Conclusions

We have shown that it is possible to produce photonic crystals with reflectance bands in the visible region by spin coating polymer multi-layers. The manufacture of these samples involves the use of a swelling based technique that enables new layers to be deposited without disrupting previous layers in the sample. The position of the optical reflectance bands that are observed in the spectra of these samples can be controlled by varying the spin speed used during deposition of the layers. The shapes and positions of the measured reflectance peaks were found to be in good agreement with the predictions of a simple optical transfer matrix model which includes the effects of diffuse polymer/polymer interfaces with interfacial widths in the 15–20 nm range. These calculations were shown to accurately predict the shape of the reflectance spectra as well as predicting the angular dependence of the wavelength/position and size of the dominant reflectance features. Chirped structures were also manufactured using an automated spin coater. The reflectance spectra obtained for these samples were also found to be in agreement with the results of transfer matrix calculations. We conclude that spin coating provides a viable route for the production of inexpensive photonic crystals with tailored optical properties.

The authors would like to thank Andrew Parnell and Richard Jones (University of Sheffield) for the use of the spectroscopic ellipsometer.

References

1. S. Kinoshita, S. Yoshioka, J. Miyazaki, Rep. Prog. Phys. **71**, 076401 (2008).
2. M. Kimura, K. Okahara, T. Miyamoto, J. Appl. Phys. **50**, 1222 (1979).
3. A.M. Adawi *et al.*, J. Appl. Phys. **99**, 054505 (2006).
4. S. Colodrero *et al.*, Adv. Mater. **21**, 764 (2009).
5. H. Takeuchi, K. Natsume, S. Suzuki, H. Sakat, Electron. Lett. **43**, 30 (2007).
6. J. Yoon, W. Lee, E.L. Thomas, NanoLett. **6**, 2211 (2006).
7. J. Yoon *et al.*, Appl. Phys. Lett. **88**, 091102 (2006).
8. K.D. Singer *et al.*, Opt. Express **16**, 10358 (2008).
9. T. Komikado, S. Yoshida, S. Umegaki, Appl. Phys. Lett. **89**, 061123 (2006).
10. P.M. Walker, J.S. Sharp, A.V. Akimov, A.J. Kent, Appl. Phys. Lett. **97**, 073106 (2010).
11. P. Vukusic, J.R. Sambles, Nature **424**, 852 (2003).
12. R. Mafouna *et al.*, Appl. Phys. Lett. **85**, 4278 (2004).
13. J. Stehr *et al.*, Adv. Mater. **15**, 1726 (2003).
14. A.M. Adawi *et al.*, Adv. Mater. **18**, 742 (2006).
15. J.S. Sharp, J.A. Forrest, Phys. Rev. Lett. **91**, 235701 (2003).
16. A. Alvarez *et al.*, Thin Solid Films **433**, 277 (2003).
17. J. Brandrup, E.H. Immergut, E.A. Grulke (Editors), *Polymer Handbook* (Wiley, New Jersey, 1999).
18. R.A.L. Jones, R.W. Richards, *Polymers at Surfaces and Interfaces* (Cambridge University Press, Cambridge, 1999).
19. R.M.A. Azzam, N.M. Bashara, *Ellipsomtery and Polarized Light* (Elsevier, London, 1987).
20. C.C. Katsidis, D.I. Siapkas, Appl. Opt. **41**, 3978 (2002).
21. D. Ennis, H. Betz, H. Ade, J. Polym. Sci., Part B: Polym. Phys. **44**, 3234 (2006).
22. H.E. Bennett, J.O. Porteus, J. Opt. Soc. Am. **51**, 123 (1961).